Applied Physics B (2025) 131:55
https://doi.org/10.1007/s00340-025-08410-5

RESEARCH

Resonant grating for wavelength and polarization selection in high-power lasers emitting in the 2-μm wavelength region

Danish Bashir[1] · Georgia Mourkioti[2] · Ayoub Boubekraoui[1] · Sergei Tomilov[3] · Mykyta Redkin[3] · Clara J. Saraceno[3] · Thomas Graf[1] · Jacob I. Mackenzie[2] · Marwan Abdou Ahmed[1]

Received: 15 December 2024 / Accepted: 3 February 2025 / Published online: 24 February 2025

Abstract

This paper presents the design, fabrication, and implementation of a single-layer resonant-reflection grating-waveguide structure (RR-GWS) optimized for laser operation in the 2 μm wavelength region. The RR-GWS was designed to function effectively across a broad spectral region ranging from 1.9 μm to 2.1 μm. Reflectance measurements confirmed the structure's wideband performance within this spectral region, with 99% resonant reflectivity. Incorporating the RR-GWS into a Ho: YAG thin-disk laser system, as a cavity folding mirror, it demonstrated very good power-handling capability and efficacy in wavelength and polarization selection. The 2 μm laser system achieved a linearly polarized output power of 36 W, with an optical efficiency of 34.6%. Additionally, the laser demonstrated a spectral bandwidth of <0.5 nm full width at half maximum, i.e., 12 times narrower than that obtained with an equivalent all-mirror reference cavity.

1 Introduction

High-power lasers operating at the 2 μm wavelength region have garnered significant interest in recent years for various scientific and industrial applications [1]. Scientifically, these lasers are pivotal for secondary source generation [2], THz spectroscopy [3], LIDAR [4], and environmental monitoring, such as detecting atmospheric gases like CO_2 [5] and H_2O [6]. In the medical field, 2 μm lasers are used for minimally invasive surgical procedures and tissue ablation due to the high absorption of their radiation in water and biological tissues [7]. Industrially, these lasers are essential for laser-based processing of polymers [8] and semiconductors, including volume processing of silicon [9], and they are increasingly used in precision machining and materials processing. Achieving high-power outputs at this wavelength typically involves coherent or spectral beam combining techniques. Spectral beam combining, in particular, demands a narrow bandwidth for each emitter or port to ensure precise wavelength selection and tuning. In this context, we introduce a single-layer resonant-reflection grating-waveguide structure (RR-GWS) [10], meticulously designed to facilitate the selection and tuning of the laser wavelength in the 2 μm spectral region. This paper provides a comprehensive analysis of the RR-GWS's design, fabrication, and integration into a high-power Ho: YAG thin-disk laser oscillator [11] to evaluate its performance. The experimental results demonstrated the RR-GWS's ability to produce linearly polarized radiation with a narrow full-width at half-maximum (FWHM) bandwidth (<0.5 nm, limited by instrument resolution), achieving an average output power of 36 W at a central wavelength of 2090 nm. The measured purity of the linear polarization of the emitted radiation exceeded 99%, and is attributed to the RR-GWS's polarization-dependent reflectance properties. Additionally, the RR-GWS's design allows for angular adjustment, which enabled tuning of the operating wavelength over a range of 28 nm around a central wavelength of 2090 nm. This tunability, combined with the high power and narrow bandwidth characteristics, underscores the RR-GWS's potential for enhancing the performance of 2 μm lasers in both scientific research and industrial processing applications.

✉ Marwan Abdou Ahmed
marwan.abdou-ahmed@ifsw.uni-stuttgart.de

1 Institut für Strahlwerkzeuge, University of Stuttgart, 70569 Stuttgart, Germany

2 Optoelectronics Research Centre, University of Southampton, Southampton SO17 1BJ, UK

3 Photonics and Ultrafast Laser Science, Ruhr Universität Bochum, Universitätsstrasse 150, 44801 Bochum, Germany

2 Design

The designed RR-GWS consisted of a structured c-cut sapphire substrate with the refractive indices n_o=1.738 and n_e=1.730 at a wavelength of $\lambda = 1970$ nm, and n_o=1.736 and n_e=1.728 at $\lambda = 2090$ nm [12]. This structured substrate was coated with a 425 nm thick Ta_2O_5 waveguide (with a refractive index of n=2.073 at 1970 nm and n=2.034 at 2090 nm). A schematic of the RR-GWS design is shown on the left of Fig. 1. The grating has a nominal period (Λ) of 984 nm, a groove depth (σ) of 200 nm and a nominal duty cycle (DC) set to 50%. The primary objective of this design was to achieve the guided-mode resonance for TE-polarized light at the two specific wavelengths of 1970 nm and 2090 nm, depending on the angle of incidence (AOI) of the radiation. The resonance at 1970 nm is suitable for Tm-doped lasers, whilst the one at 2090 nm is suitable for Ho-doped lasers. The guided-mode resonances at 1970 nm and 2090 nm were achieved at the AOIs of 12.7° and 20.6°, respectively. As depicted in Fig. 1 (right), a theoretical reflectance of R_{TE} = 99.99% for TE-polarization and $R_{TM} \approx$ 6% for TM-polarization was calculated for both the wavelengths. Furthermore, the FWHM spectral bandwidths of the resonance peaks were calculated to be approximately $\Delta\lambda \approx 23.25$ nm at 1970 nm and $\Delta\lambda \approx 21.5$ nm at 2090 nm. The width of the resonances at a reflectance level of 95% were calculated to be 5.1 nm at 1970 nm and 4.75 nm at 2090 nm. The combination of the large difference between the reflectance for the TE- and the TM-polarized radiation with the narrow spectral bandwidths of the resonances collectively ensures the polarization and wavelength selectivity of our device.

3 Fabrication and characterization

Electron-beam lithography was employed to pattern the binary grating structure on a 650-µm-thick c-cut sapphire substrate. Prior to patterning, the substrate was coated with a 50 nm thick chromium (Cr) layer and a 400 nm thick SiO_2 layer, which served as etching masks. The grating was then etched onto the sapphire substrate using inductively coupled plasma (ICP) tools (Oxford Plasmalab 100, Plasmalab 80, and OPT Sys100 ICP380-Plasmalab). A 425 nm thick layer of Ta_2O_5 was subsequently deposited on top of the structured substrate using RF magnetron sputtering (Plasmalab 400+, Oxford Instruments Plasma Technology) from a dense tantalum ceramic target.

An atomic force microscope (AFM) was used to analyze the grating profile of the fabricated RR-GWS sample. As illustrated in Fig. 2, the AFM measurements revealed that the grating profile had a trapezoidal shape instead of the intended rectangular design. The side wall angle (SWA) was measured to be 29° relative to the vertical plane, and the etch depth was found to be 225 nm. These deviations in the grating parameters are mainly attributed to fabrication tolerances. Furthermore, the AFM profile indicates that within the grating grooves there is an approximately 5 nm high 'mound' across the approximately 200 nm wide base, which appears to be, there is an approximately 5 nm high 'mound' across the approximately 200 nm wide base, which appears to be a build-up of Ta_2O_5 ostensibly due to the structure's geometry and directionality of the deposition plasma.

To characterize the performance of the fabricated RR-GWS, the wavelength- and polarization-dependent reflectivity was measured with the setup illustrated in Fig. 3.

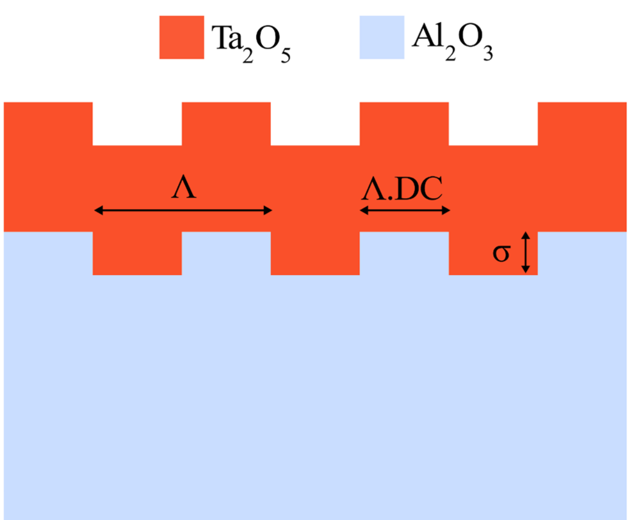

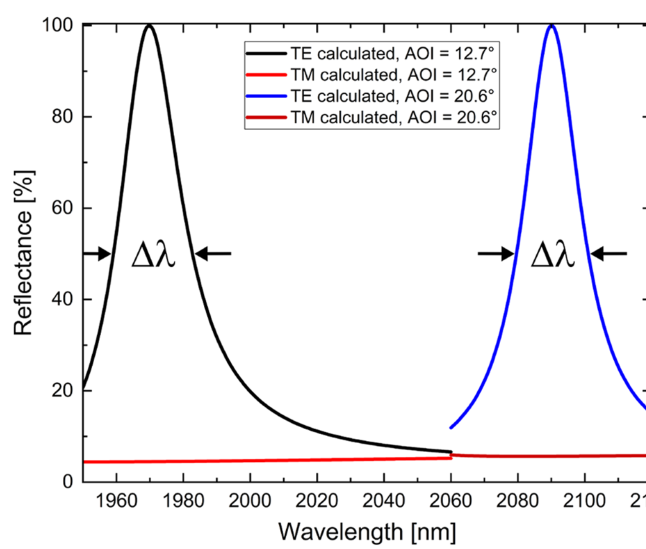

Fig. 1 Left) Schematic of the device. The grating is etched into sapphire with a period of Λ=984 nm, a groove depth of σ=200 nm, and a duty-cycle (DC) of 50%. A 425 nm-thick layer of Ta_2O_5 is deposited on top of the etched grating. **Right)** Calculated spectral reflectance for TE and TM polarized radiation at AOI's of 12.7° and 20.6°

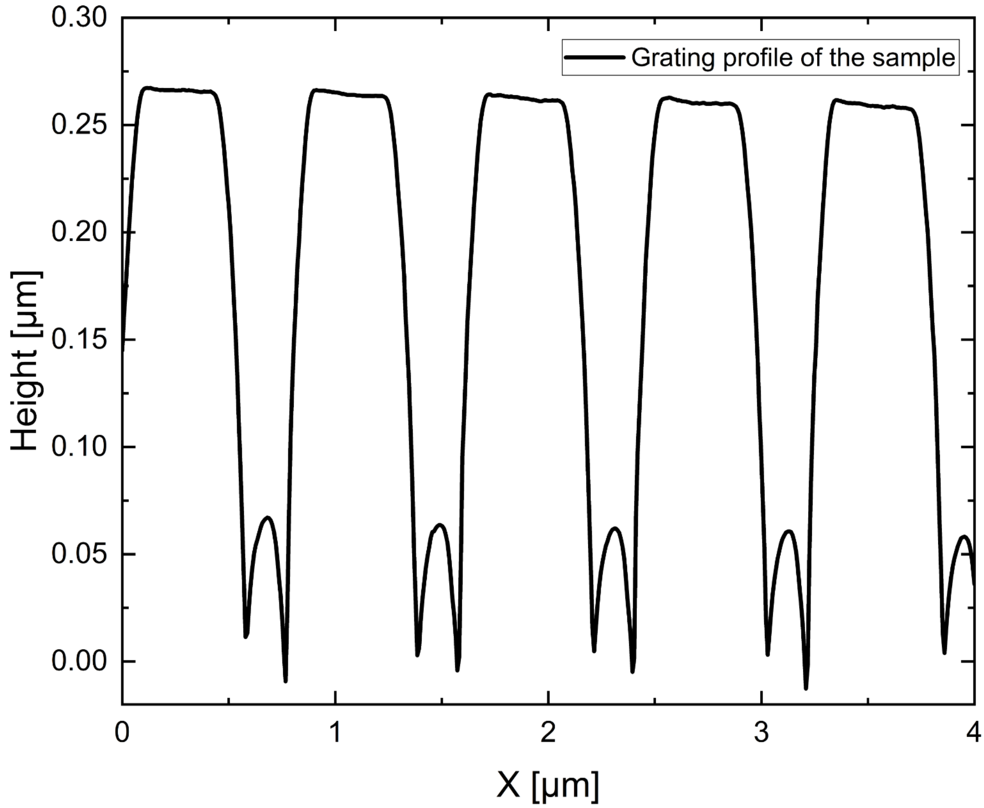

Fig. 2 AFM measurement of the grating profile after deposition of the Ta_2O_5 layer

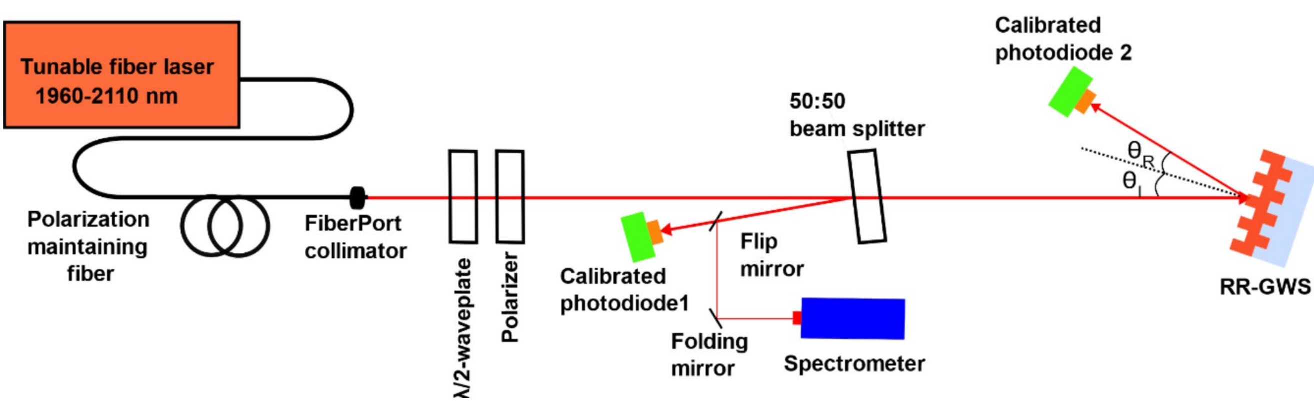

Fig. 3 Schematic of the reflectivity setup

A Thulium-Holmium (Tm-Ho) co-doped tunable fiber laser was used, providing a narrow bandwidth of <0.5 nm (FWHM, limited by instrument resolution), with a tuning range from 1960 nm to 2110 nm. A combination of a half-wave plate and a polarizer were used to set the desired polarization state and intensity of the incident beam. A 50:50 pellicle beam splitter was introduced in the beam path to separate the reference (reflected) and the probe (transmitted) beams. Two calibrated integrating spheres with photodiode sensors were employed to simultaneously monitor the power of the reference and the probe beam reflected from the RR-GWS. The reflectance of the RR-GWS was determined by comparing the power readings from the two photodiode sensors.

A reflectance of $R_{TE} = 98.7 \pm 0.3\%$ and of $R_{TM} = 10 \pm 7\%$ was measured at the resonance angles of incidence of 12.8° and 20.7° for the wavelengths of 1970 nm and 2090 nm, respectively. The relatively strong modulation of the measured R_{TM} is attributed to additional interference with the reflection from the un-coated back surface of the relatively thin substrate, which was not accounted for in the simulation. The spectral bandwidths of the R_{TE} peaks were measured to be $\Delta\lambda \approx 23.8$ nm (FWHM) at the wavelength of 1970 nm and $\Delta\lambda \approx 22.3$ nm (FWHM) at 2090 nm. The experimentally determined resonance angles and spectral

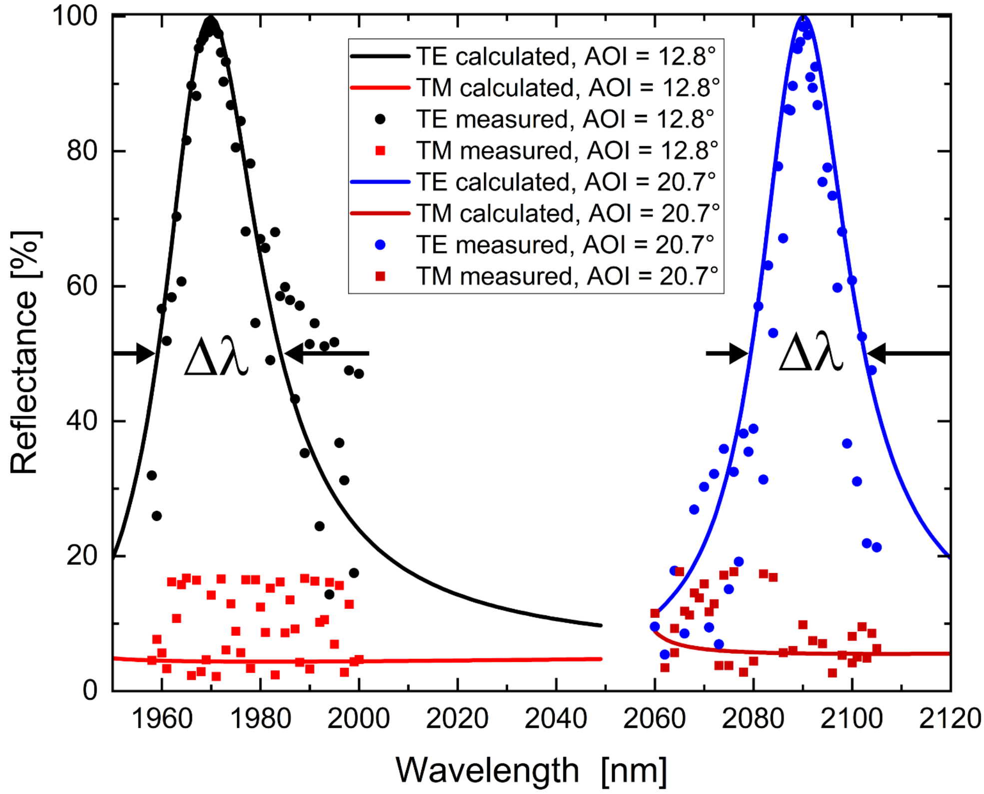

Fig. 4 Measured reflectance data points at an AOI of 12.8° (1970-nm resonance) and 20.7° (2090-nm resonance), overlaid with simulation results (lines), which incorporated the AFM measurements of the grating profile

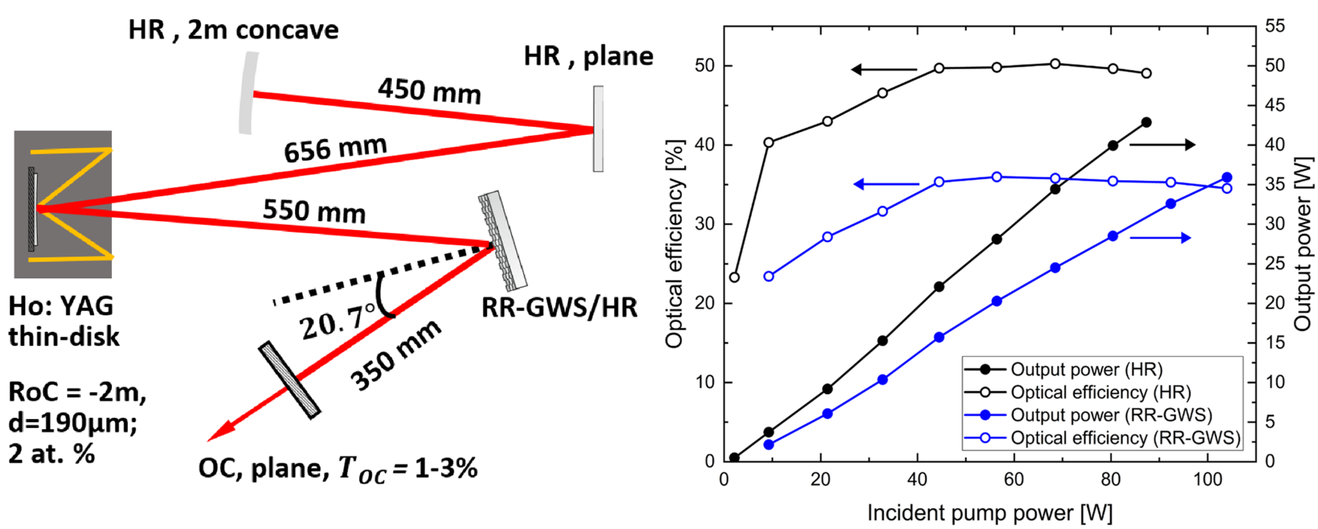

Fig. 5 Left) Ho: YAG thin-disk laser resonator setup. **Right)** Comparison of laser performance characteristics between the resonator using a plane HR folding mirror and the resonator using the RR-GWS as the folding mirror

bandwidths are slightly shifted compared to the designed values, primarily due to minor deviations in the opto-geometrical parameters of the grating and waveguide, as indicated by the AFM measurements. Figure 4 shows the good agreement between the measured and calculated reflectance spectra, when the grating profile measured by the AFM was used for the numerical calculation.

4 Intracavity Laser Test

The performance of the fabricated RR-GWS was tested by implementing it as a folding mirror in a Ho: YAG thin-disk laser cavity, Fig. 5 (left). A resonator was set up that oscillated in a near to transverse fundamental-mode operation, cf. Figure 5 (left). It comprised a concave high-reflectance (HR) end mirror with a radius of curvature (RoC) of 2 m, a plane HR folding mirror, a Ho: YAG thin-disk crystal, the

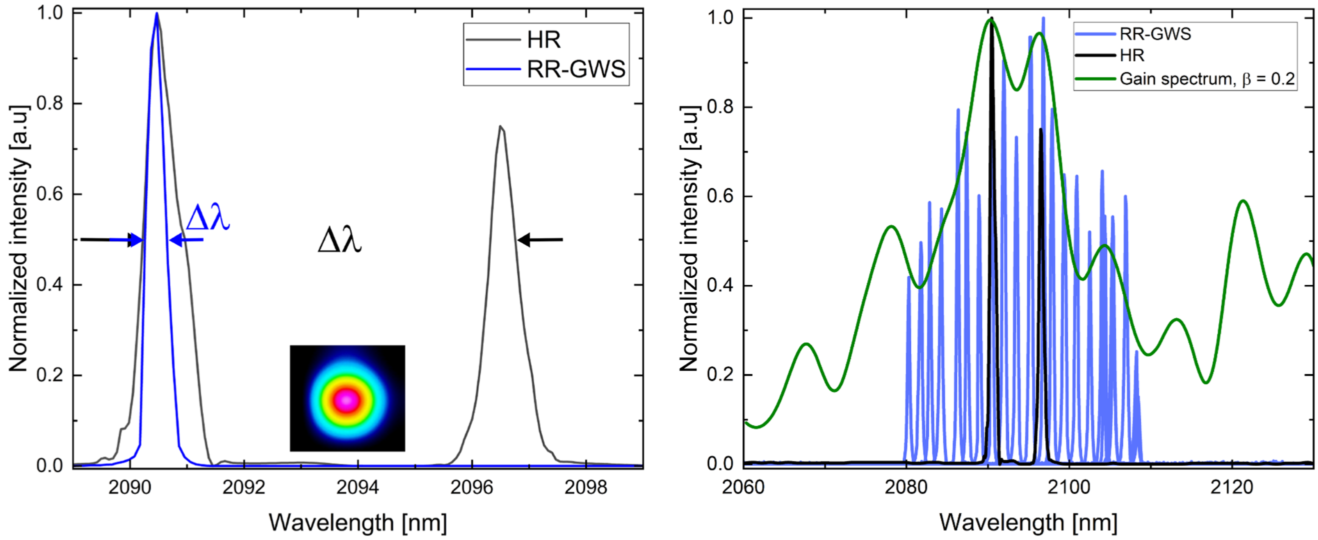

Fig. 6 **Left)** Emission spectra recorded at 30 W output power, showing a reduction in bandwidth (Δλ) from 6 nm with the plane HR mirror to less than 0.5 nm with the RR-GWS configuration. The inset displays the corresponding laser beam's intensity distribution with the RWG in the resonator. **Right)** Wavelength tuning range from 2080 nm to 2108 nm achieved by adjusting the AOIs to the RR-GWS. A tuning range of $\Delta\lambda_T = 28$ nm was demonstrated

RR-GWS, and a plane output coupler (OC) with a transmission of 1 to 3%. For comparison of the resulting laser performance, the RR-GWS could be replaced by a plane HR mirror. The Ho: YAG thin disk, with a thickness of 190 µm and a doping concentration of 2 at.%, was glued to a water-cooled diamond heat sink. Its RoC was determined to be -2 m. The assembled disk was integrated into a pumping module, where 36 reflections of the pump radiation through the laser crystal were used. A commercial Tm: fiber laser with a wavelength of 1908 nm and a maximum power of 209 W was used for pumping. As shown in Fig. 5 (right), the laser performance was first assessed using the reference HR plane folding mirror instead of the RR-GWS and an OC with a transmission of 3%, resulting in a maximum output power of 43 W and an optical efficiency of 49.1% at 87.4 W of incident pump power. Further increase of the pump power was avoided to prevent damage of the Tm: fiber laser that could potentially be caused by the back reflection of the unabsorbed pump power. Moreover, it was limited by the relatively high increase of the surface temperature of the disk. Interchanging the HR folding mirror with the RR-GWS reduced the output power to 30 W, corresponding to an optical efficiency of 34.3%. This reduction can primarily be attributed to the lower reflectance of the RR-GWS. Increasing the pump power to 104 W with the RR-GWS configuration resulted in an output power of 36 W, corresponding to an optical efficiency of 34.6%.

Figure 6 (left) presents the measured emission spectra. Implementing the RR-GWS as one of the cavity mirrors of the resonator led to a substantial reduction of the laser emission's spectral bandwidth to $\Delta\lambda < 0.5$ nm. It is worth mentioning that the spectral bandwidth measurement was limited by the spectrometer's resolution at this wavelength. Specifically, the bandwidth decreased from $\Delta\lambda \approx 6$ nm, which was observed with the HR folding mirror, taking into account the two emission peaks arising due to the gain distribution for Ho: YAG, as depicted in Fig. 6 (right). Moreover, the wavelength tuning capability of the RR-GWS-laser was demonstrated by adjusting the AOI on the RR-GWS in combination with a 1%-transmission OC. This adjustment allowed the operating wavelength to be tuned from 2080 nm to 2108 nm, i.e., a tuning range of $\Delta\lambda_T = 28$ nm, limited by the gain bandwidth of the Ho: YAG active medium.

A critical factor in the performance of RR-GWS is their capacity to withstand high average powers. Therefore, the surface temperature of the RR-GWS was monitored using a thermal imaging camera (Jenoptik VarioCAM HD 1024 × 768) during laser operation. During use, the RR-GWS was mounted on a water-cooled copper holder, with a 7 mm × 7 mm through-hole behind the central region of the sample. With an output coupling transmissivity of 1% and an output power of 16 W, the intra-cavity power density on the RR-GWS was calculated to be 82.4 kW/cm², assuming a second-moments beam diameter of 2.36 mm derived from the actual resonator model. Under these conditions, the measured peak surface temperature reached 75.4 °C, representing a temperature increase of 51.4 K, corresponding to a power density specific increase of 0.57 K/(kW·cm²). This rate is approximately 2.2 times higher than that reported in [10] for a similar RR-GWS used in thin-disk laser operated at a wavelength of 1 µm. It is hypothesized that the primary factor contributing to this increased temperature rise is a longer propagation length of the radiation in the waveguide. Using the method described in [13], the propagation length was estimated to be 42 µm, compared to 13 µm reported for the RR-GWS in [10]. Additionally, finite absorption in the Ta_2O_5 film at a wavelength of 2 microns and the larger interaction volume are anticipated to contribute to a higher thermal load in this RR-GWS sample.

The degree of linear polarization (DOLP) was quantitatively measured using a Glan-Taylor polarizer to be greater than 99%, indicating a highly polarized laser output. A scanning slit beam profiler (DataRay Beam'R2) was used to assess the beam quality. The beam propagation factor was determined from the caustic after a focusing lens. When using the RR-GWS at an output power of P_{out} = 30 W, which corresponds to an intra-cavity power of P_{IC} = 1.09 kW, the beam propagation factor was measured to be $M^2_x = 1.39$ and $M^2_y = 1.34$. Notably, the reference cavity with the HR end mirror showed a higher beam propagation factor of $M^2 = 1.8$. This is attributed to the slightly different cavity design compared to that using the RR-GWS sample. In fact, a slight curvature in the mounted RR-GWS accounts for the subtle change in the cavity mode and improved beam propagation factor.

5 Conclusion

In conclusion, we have successfully showcased the design, fabrication, and initial integration of an intra-cavity resonant-reflection grating-waveguide structure (RR-GWS) into a high-power 2 µm Ho: YAG thin-disk laser system. The RR-GWS effectively defined the wavelength and polarization state, achieving a maximum linearly polarized output power of 36-W, with an optical efficiency of 34.6%, in near fundamental-mode operation. With angle-tuning of the RR-GWS the laser exhibited tunable operation across wavelengths ranging from 2080 nm to 2108 nm, with a narrow spectral bandwidth of <0.5 nm FWHM. This first high-power 2-µm laser demonstration highlights the potential of the RR-GWS for applications requiring precise wavelength control, spectral purity, and linearly polarized output. Future work will focus on optimizing the RR-GWS for higher reflectance and thermal-handling capacity, as well as exploring grating-waveguide structures based on resonant-diffraction mechanism [14, 15].

Acknowledgements The authors acknowledge ALPhANOV and University of Bordeaux for providing the tunable laser source for the characterization of the RR-GWS.

Author contributions D.B. and M.A.A. provided the design of RR-GWS. G.M. developed the fabrication process of the RR-GWS. D.B. conducted the spectroscopic characterization of the RR-GWS. A.B., S.T. and M.R. conducted the laser experiments. D.B. formulated the first draft of the manuscript. C.J.S., J.M., T.G. and M.A.A. assisted in the preparation of the manuscript. D.B., G.M., A.B. and S.T. contributed equally to the experimental results presented in this paper. All authors reviewed the manuscript and provided their respective inputs.

Funding Open Access funding enabled and organized by Projekt DEAL.
This project has received funding from the European Union's Horizon 2020 research and innovation programme under the Marie Skłodowska-Curie grant agreement No.813159. JM also acknowledges the U.K. Engineering and Physical Sciences Research Council (EPSRC) for financial support via the grant EP/P027644/1.

Data availability No datasets were generated or analysed during the current study.

Declarations

Disclosures JM declares that he is Editor in Chief for Applied Physics B: Lasers and Optics, however this manuscript has undergone independent peer review, exactly as would any other paper submitted to the journal, without his involvement.

Competing interests The authors declare no competing interests.

References

1. K. Scholle, S. Lamrini, P.Koopmann and P.Fuhrberg, 2-µm laser sources and their possible applications, Frontiers in Guided Wave Optics and Optoelectronics, Bishnu Pal (Ed.), ISBN: 978-953-7619-82-4, InTech (2010)
2. J. Zhang, K. Fai Mak, N. Nagl, M. Seidel, D. Bauer, D. Sutter, V. Pervak, F. Krausz, O. Pronin, Multi-mw, few-cycle mid-infrared continuum spanning from 500 to 2250 cm^{-1}. Light Sci. Appl. **7**, 1718 (2018)
3. R.A. Lewis, A review of terahertz sources. J. Phys. D: Appl. Phys. **47**, 374001 (2014)
4. K. Li, C. Niu, C. Wu, Y. Yu, Y. Ma, Development of a 2-µm solid-state laser for Lidar in the past decade. Sensors. **23**, 7024 (2023). https://doi.org/10.3390/s23167024
5. A. Pal, R. Sen, K. Bremer, S. Yao, E. Lewis, T. Sun, K.T.V. Grattan, All-fiber tunable laser in the 2 µm region, designed for CO_2 detection. Appl. Opt. **51**, 7011–7015 (2012)
6. H. Iwai, M. Aoki, Evaluation of a coherent 2-µm differential absorption lidar for water vapor and radial wind velocity measurements. Opt. Express. **31**, 13817–13836 (2023)
7. G.C. Gottlob, G.E. Kopchok, S.K. Peng, M. Tabbara, D. Cavaye, R.A. White, Holmium:YAG laser ablation of human intervertebral

disc: preliminary evaluation. Lasers Surg. Med. **12**, 86–91 (1992). https://doi.org/10.1002/lsm.1900120113
8. I. Mingareev, F. Weirauch, A. Olowinsky, L. Shah, P. Kadwani, M. Richardson, Welding of polymers using a 2 μm thulium fiber laser. Opt. Laser Technol. **44**, 2095–2099 (2012)
9. R. Wang, S. Sprengel, M. Muneeb, G. Boehm, R. Baets, M.C. Amann, G. Roelkens, 2 μm wavelength range InP-based type-II quantum well photodiodes heterogeneously integrated on silicon photonic integrated circuits. Opt. Express. **23**, 26834–26841 (2015)
10. D. Bashir, A. Boubekraoui, G. Mourkioti, F. Li, P. Karvinen, M. Kuittinen, J.I. Mackenzie, T. Graf, M.A. Ahmed, Sapphire-based resonant waveguide-grating mirrors: advancing their intra-cavity power density capability. Appl. Phys. B **130**, 4 (2024)
11. S. Tomilov, M. Hoffmann, Y. Wang, C.J. Saraceno, Moving towards high-power thin-disk lasers in the 2 μm wavelength range. J. Phys. Photonics. **3**, 022002 (2021)
12. I.H. Malitson, J. Opt. Soc. Am. **52**, 1377–1379 (1962)
13. V.A. Sychugov, A.V. Tishchenko, N.M. Lyndin, O. Parriaux, Spectral and angular sensitivities of resonant diffraction in deep dielectric reflection gratings. Sens. Actuators B Chem. **39**(1–3), 360–364 (1997)
14. M. Rumpel, A. Voss, M. Moeller, F. Habel, C. Moormann, M. Schacht, T. Graf, M.A. Ahmed, Linearly polarized, narrow-linewidth, and tunable yb: YAG thin-disk laser. Opt. Lett. **37**, 4188–4190 (2012)
15. N. Destouches, A. Tishchenko, J. Pommier, S. Reynaud, O. Parriaux, S. Tonchev, M.A. Ahmed, 99% efficiency measured in the −1st order of a resonant grating. Opt. Express. **13**, 3230–3235 (2005)